Supplement of Hydrol. Earth Syst. Sci., 25, 5859–5878, 2021
https://doi.org/10.5194/hess-25-5859-2021-supplement

Hydrology and Earth System Sciences
Open Access
EGU

Supplement of

Large-scale sensitivities of groundwater and surface water to groundwater withdrawal

Marc F. P. Bierkens et al.

Correspondence to: Marc F. P. Bierkens (m.f.p.bierkens@uu.nl)

Supplementary Table S1. Sensitivity of global results to parameters C (stream-aquifer resistance) and d (stream bottom elevation). Sensitivities are expressed as relative change in the output variable V per relative unit change in the parameter (C or d).

Variable V	Sensitivity $(\frac{\partial V}{V})/(\frac{\partial C}{C})$	Sensitivity $(\frac{\partial V}{V})/(\frac{\partial d}{d})$
q_{crit} (Sutanudjaja et al., 2018)	$6.81 \cdot 10^{-3}$ (0.000 -0.459)	-
q_{crit} (Cuthbert et al., 2018)	$5.23 \cdot 10^{-5}$ (0.000 -0.890)	-
t_{crit} (Sutanudjaja et al., 2018)	0.185 ($2.61 \cdot 10^{-6}$-1.39)	0.264 ($1.18 \cdot 10^{-5}$-34.3)
t_{crit} (Cuthbert et al., 2018)	1.05 ($7.71 \cdot 10^{-3}$-1.09)	$8.50 \cdot 10^{-3}$ ($6.65 \cdot 10^{-6}$-3.83)
$q \leq q_{\text{crit}}$		
$dh=h(0)-h(\infty)$	0.371 (0.000–1.05)	0.000 (0.000-0.000)
$dQ=Q(0)-Q(\infty)$	$1.31 \cdot 10^{-11}$ (0.000 -$1.48 \cdot 10^{-4}$)	$2.19 \cdot 10^{-13}$ (0.00-0.270)
$t_{ef} = nC/(1-\beta)$	0.230 ($6.83 \cdot 10^{-5}$-0.952)	-
$q > q_{\text{crit}}$ and $h < d$		
dh/dt	$3.43 \cdot 10^{-8}$ (0.000 -0.399)	-
$dQ=Q(0)-Q(\infty)$	$8.89 \cdot 10^{-3}$ ($5.93 \cdot 10^{-9}$-0.482)	$2.22 \cdot 10^{-15}$ (0.000-$9.77 \cdot 10^{-10}$)
$f_{cap} = q_{cap}/q$	0.000 (0.000-0.000)	-

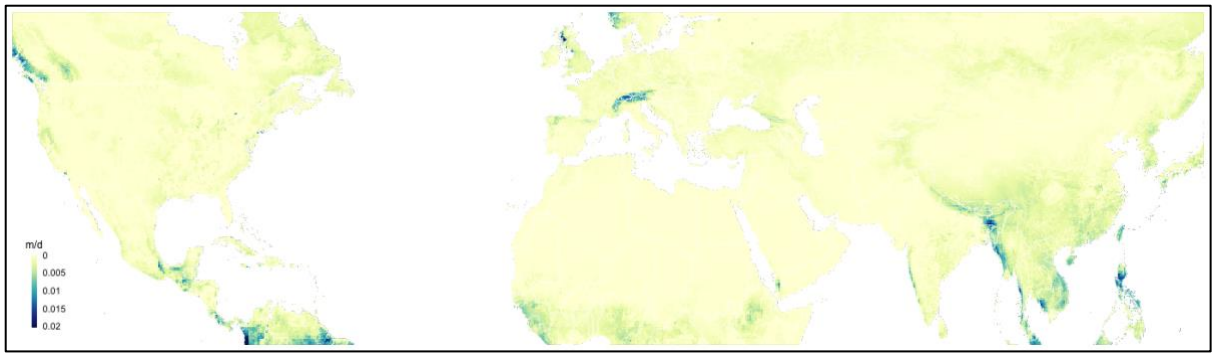

Supplementary Figure S1. Parameters used in global analyses (Sutanudjaja et al., 2018): q_s, sum of surface runoff and interflow (m d^{-1})

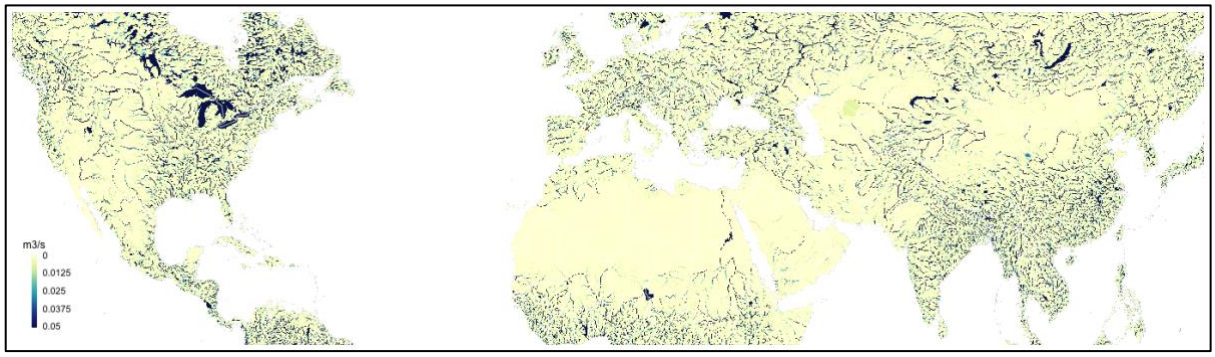

Supplementary Figure S2. Parameters used in global analyses (Sutanudjaja et al., 2018): Q_i, upstream discharge (m^3 s^{-1})

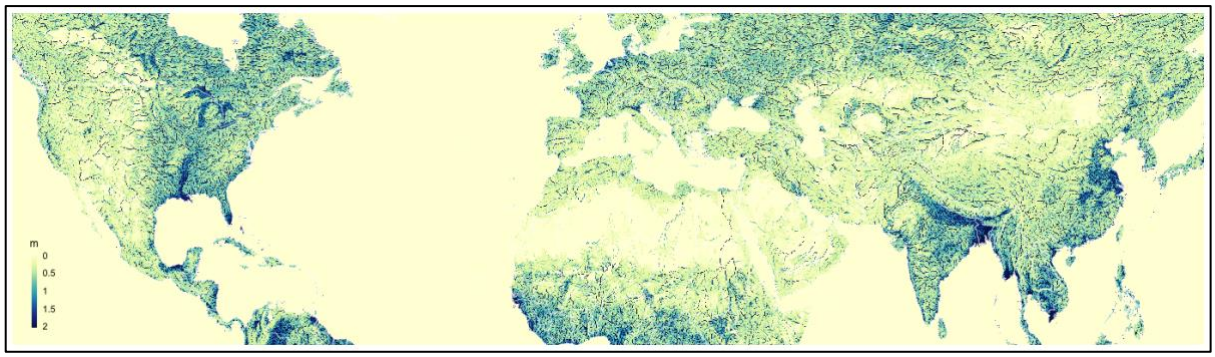

Supplementary Figure S3. Parameters used in global analyses (Sutanudjaja et al., 2018): Stream depth (m) based on bankfull discharge. Surface elevation minus stream depth results in stream bottom elevation d.

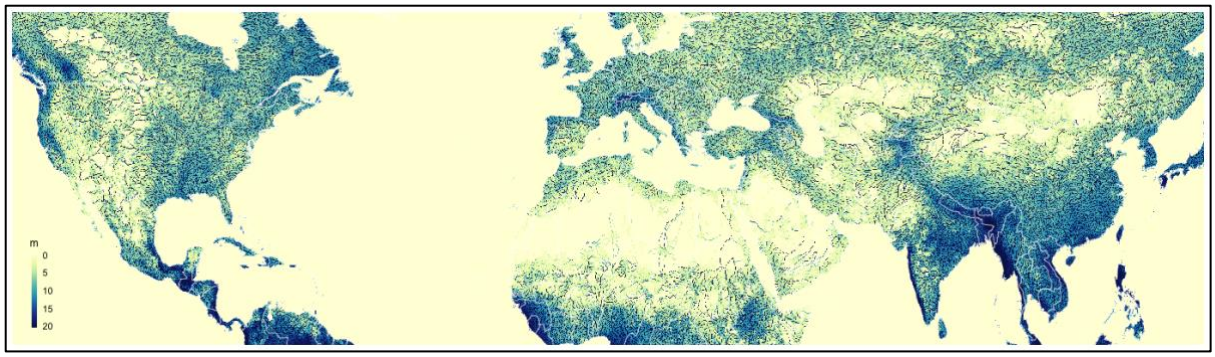

Supplementary Figure S4. Parameters used in global analyses (Sutanudjaja et al., 2018): W, stream width (m) based on bankfull discharge.

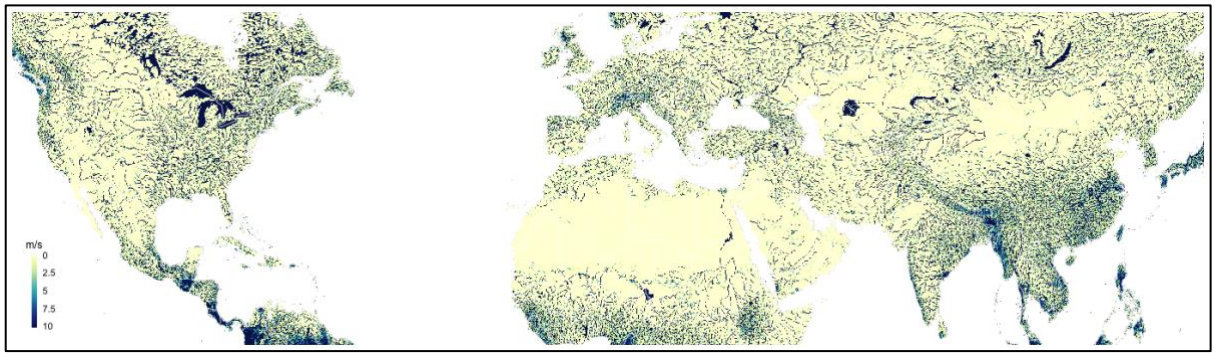

Supplementary Figure S5. Parameters used in global analyses (Sutanudjaja et al., 2018): v, water velocity (m s^{-1}), calculated from bankfull discharge and stream depth assuming v to be dependent on terrain slope only.

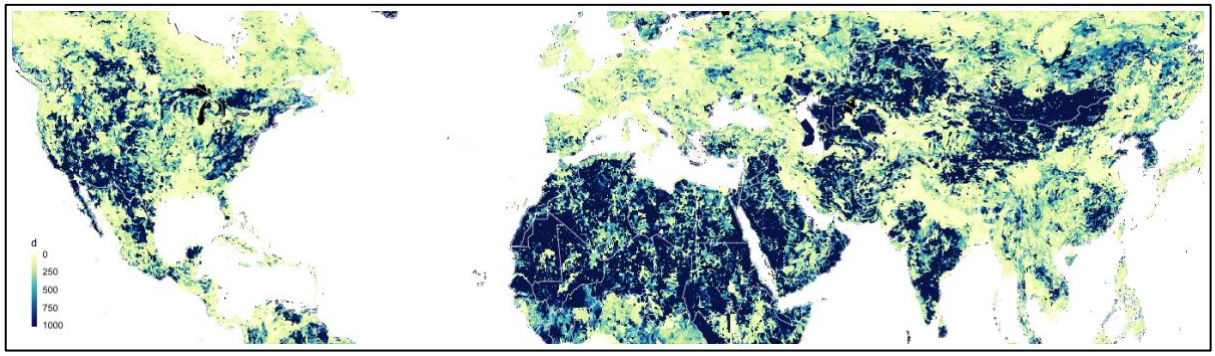

Supplementary Figure S6. Parameters used in global analyses (Sutanudjaja et al., 2018): C = J/n (d), with J the characteristic response time of the lower reservoir in PCR-GLOBWB.

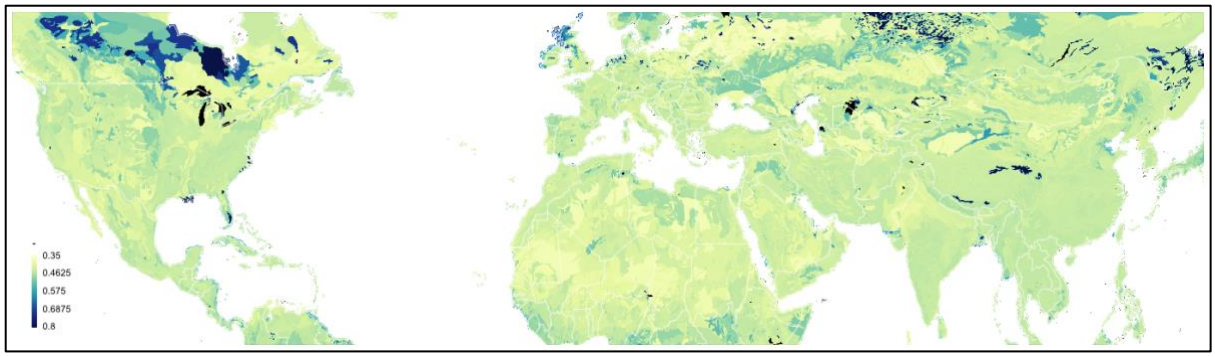

Supplementary Figure S7. Parameters used in global analyses (Sutanudjaja et al., 2018): n, porosity values (-) from the groundwater reservoir in PCR-GLOBWB.

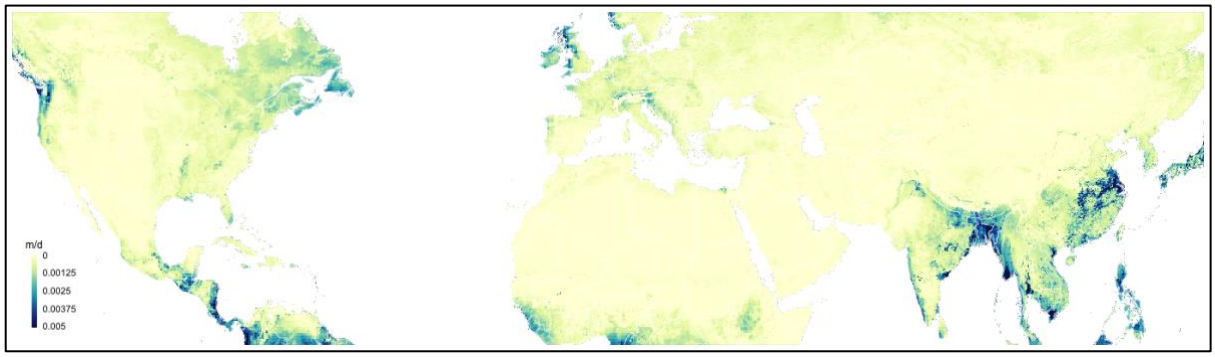

Supplementary Figure S8. Parameters used in global analyses (Sutanudjaja et al., 2018): r, net recharge (recharge minus capillary rise) (m d^{-1}).

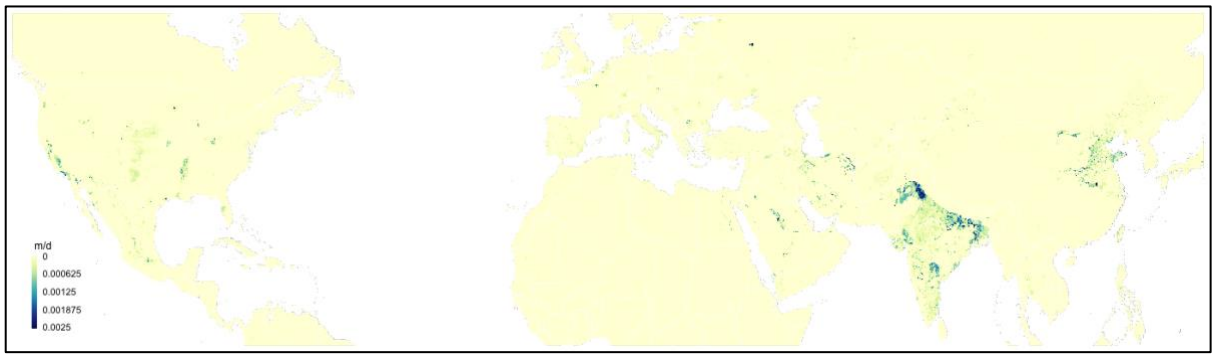

Supplementary Figure S9. Parameters used in global analyses (Sutanudjaja et al., 2018): q, groundwater pumping rate (m d^{-1}).

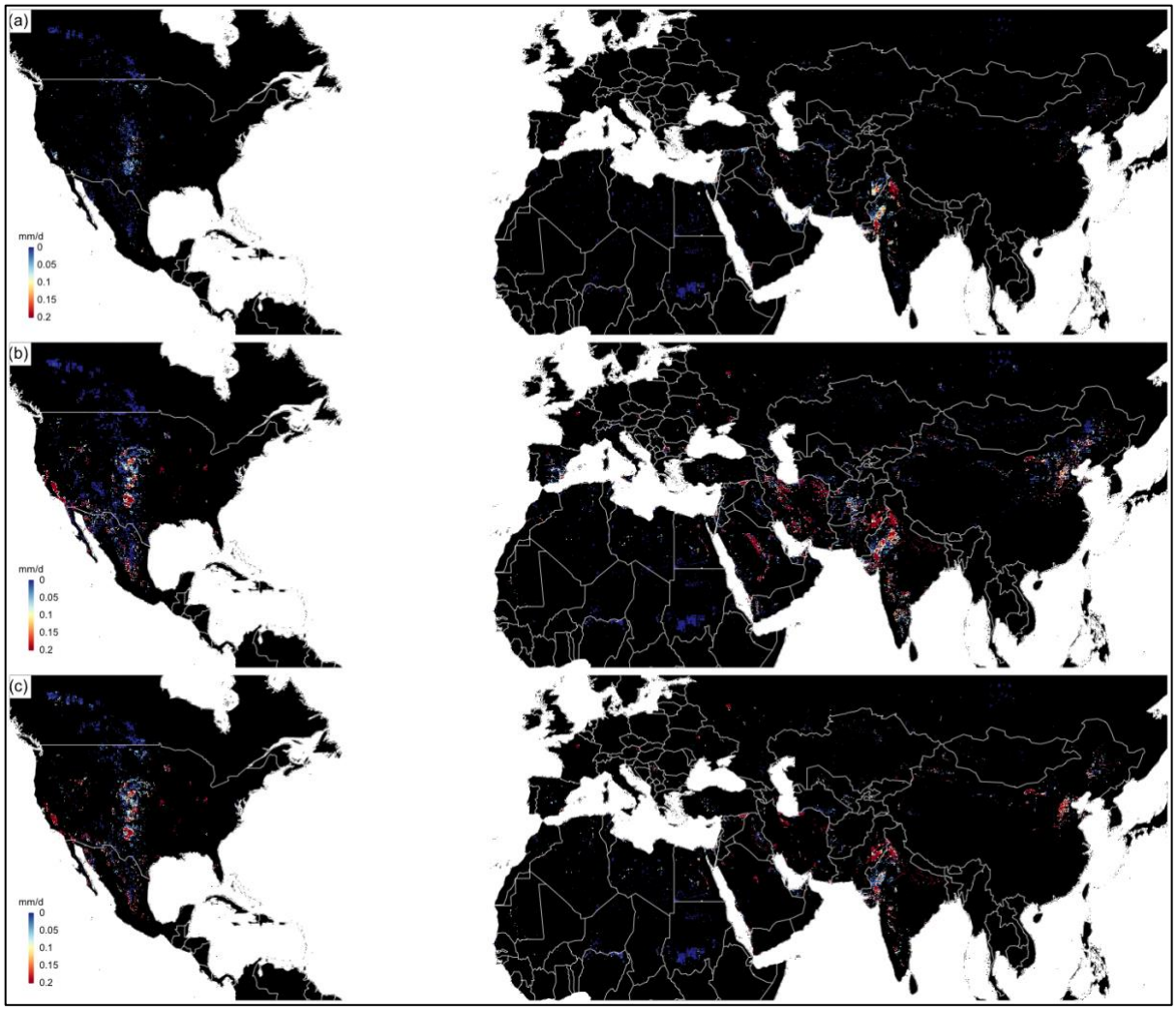

Supplementary Figure S10. Comparison of average groundwater head decline rates (mm d^{-1}) over the period 2000-2015 by De Graaf et al. (2019) with estimates over the same period with the analytical framework; comparisons are limited to areas where $q > q_{crit}$ (assuming $t > t_{crit}$); (a) results from De Graaf et al. (2019); (b) estimates from the analytical framework ; (c) absolute differences |b-a|.

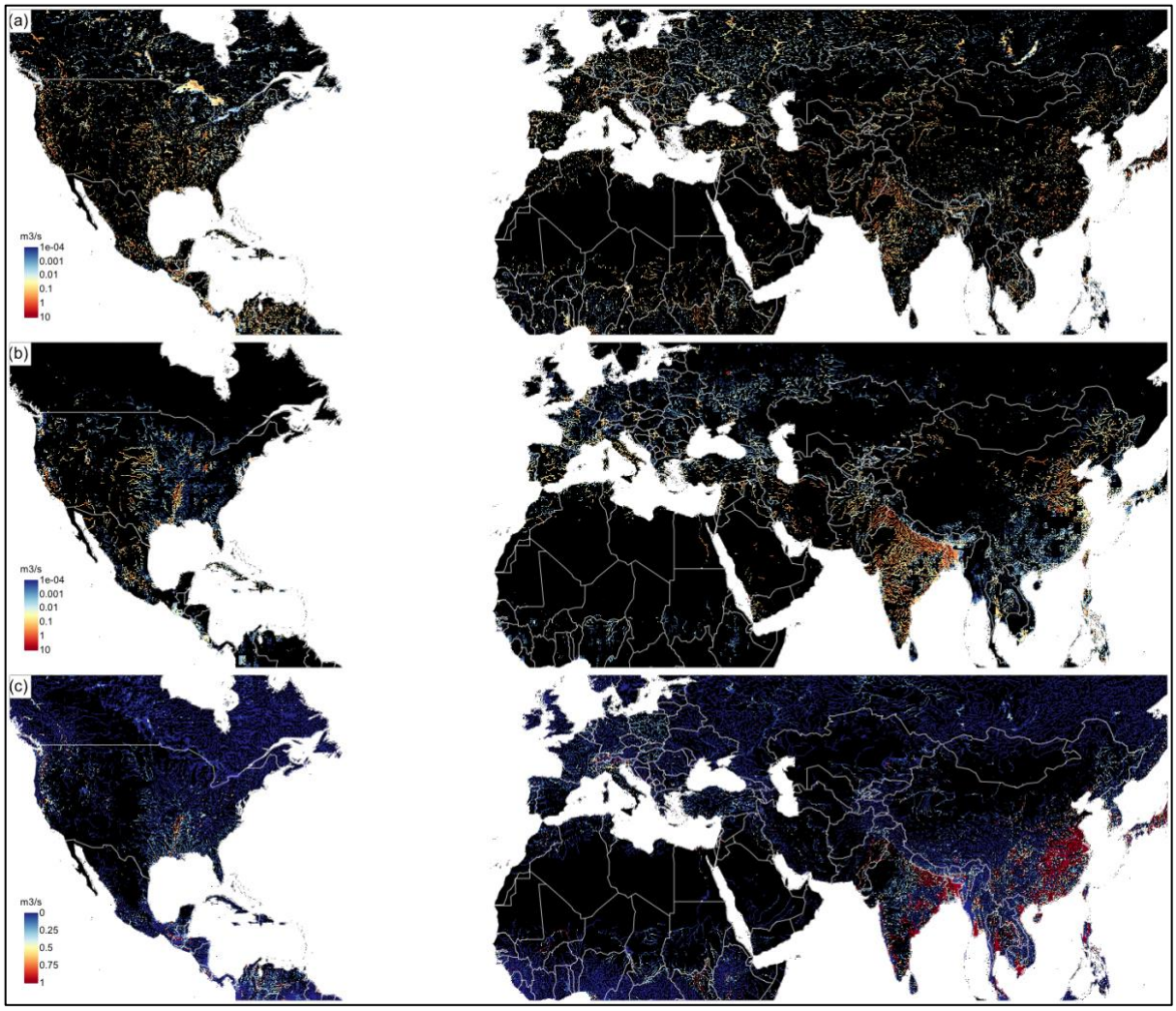

*Supplementary Figure S11. Comparison of total streamflow depletion ($m^3\ s^{-1}$) over the period 2000-2015 by De Graaf et al. (2019) with the estimates over the same period with the analytical framework (*assuming $q > q_{crit,}\ t > t_{crit}$ or $q < q_{crit,}\ t >> t_{ef}$*); (a) results from De Graaf et al. (2019); (b) estimates from the analytical framework; (c) absolute differences |b-a|.*

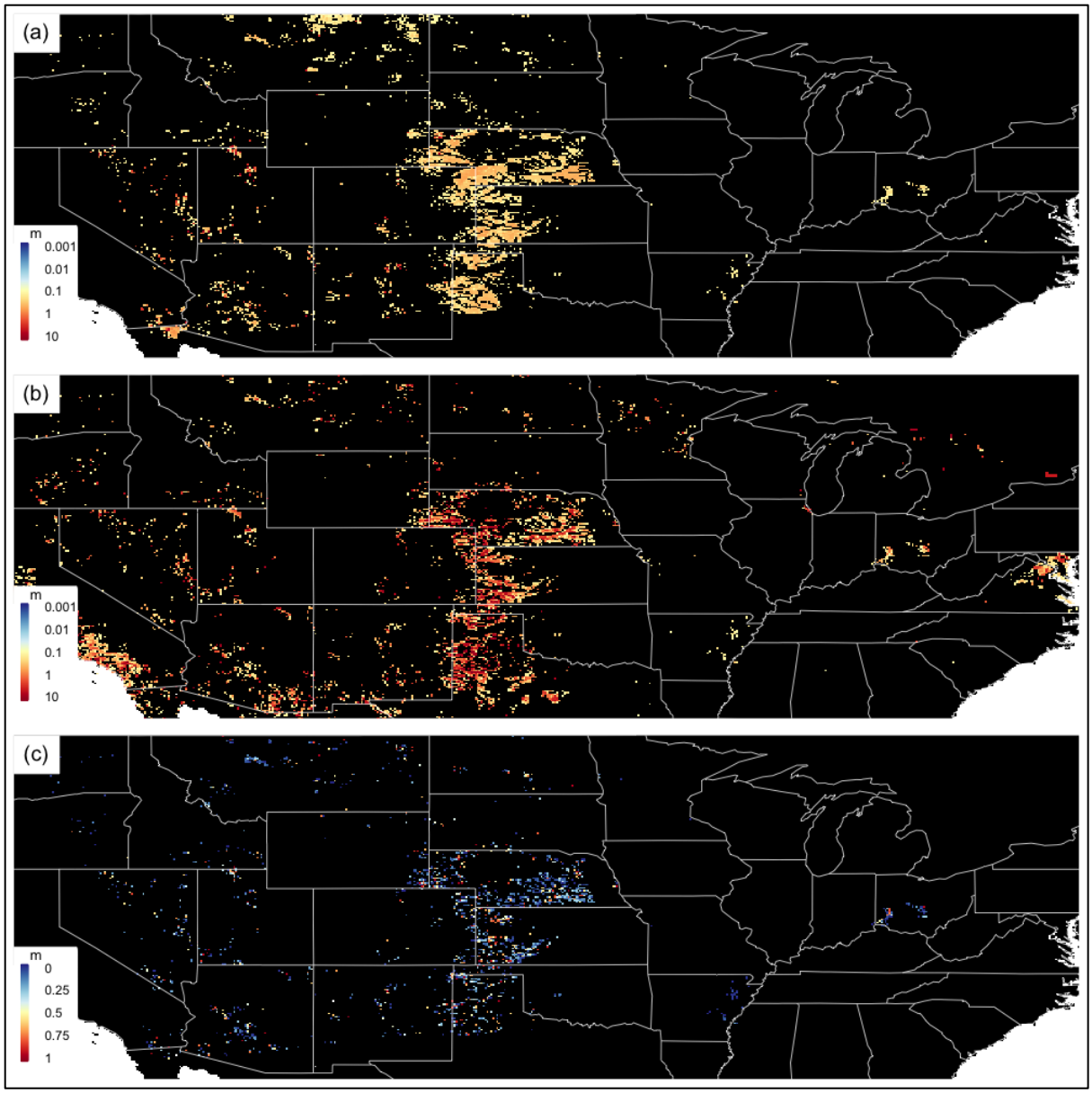

Supplementary Figure S12. Comparison of groundwater depletion (groundwater removed from storage) (m) since predevelopment (1900-2008) as simulated with ParFlow-CLM by Condon and Maxwell (2019) with the estimates with the analytical framework; comparisons are limited to areas where $q > q_{crit}$ (assuming, $t > t_{crit}$); *(a) results from Condon and Maxwell (2019); (b) estimates from the analytical framework; (c) absolute differences |b-a|.*

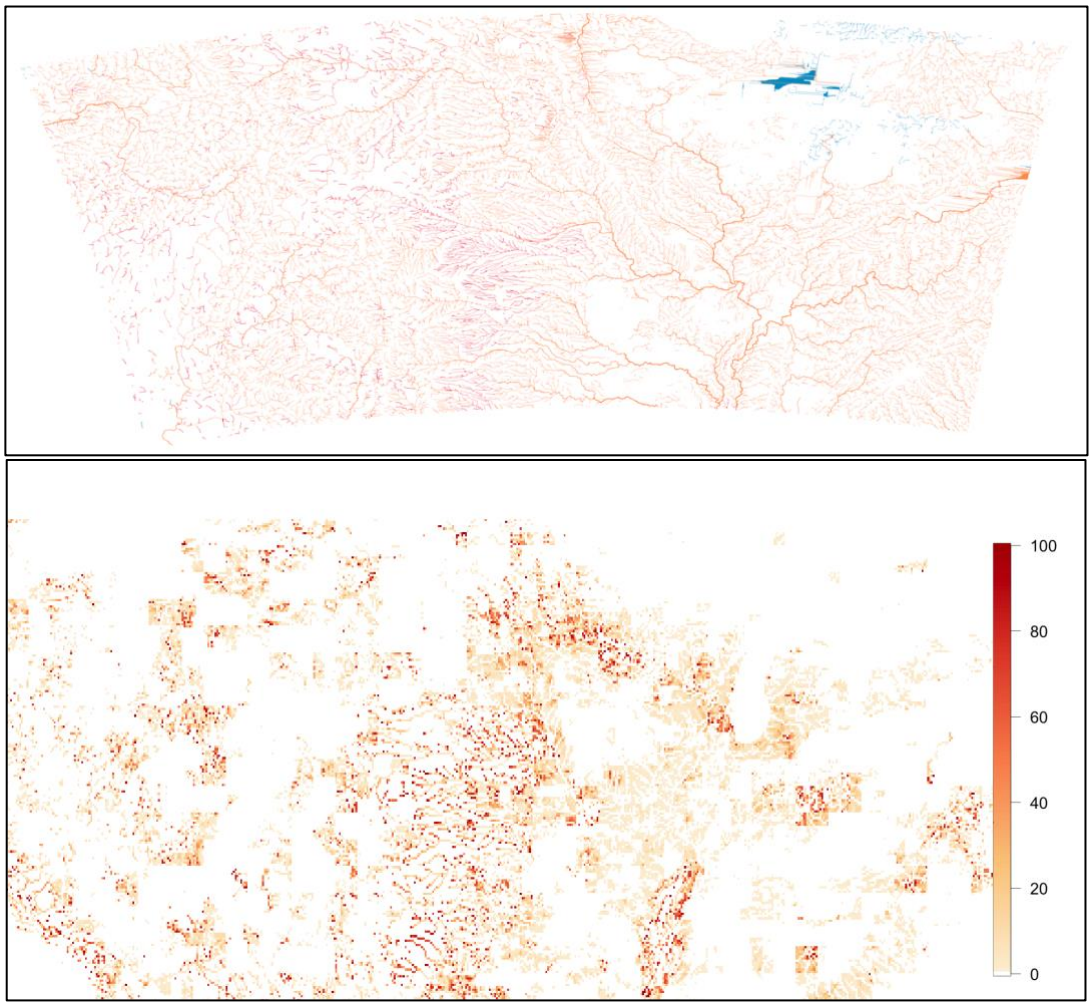

*Supplementary Figure S13. Comparison of streamflow depletion (% change in discharge) since predevelopment (1900-2008) as simulated with ParFlow-CLM by Condon and Maxwell (2019) with the estimates with the analytical framework (*assuming $q > q_{crit,}$ $t > t_{crit}$ or $q < q_{crit,}$ $t >> t_{ef}$*); top: results from Condon and Maxwell (2019); bottom: estimates from the analytical framework; note that the Condon and Maxwell results represent cumulative dQ as fraction of Q, whereas the results from the analytical framework represent marginal dQ as a fraction of Q; this makes the results only comparable for the headwaters.*

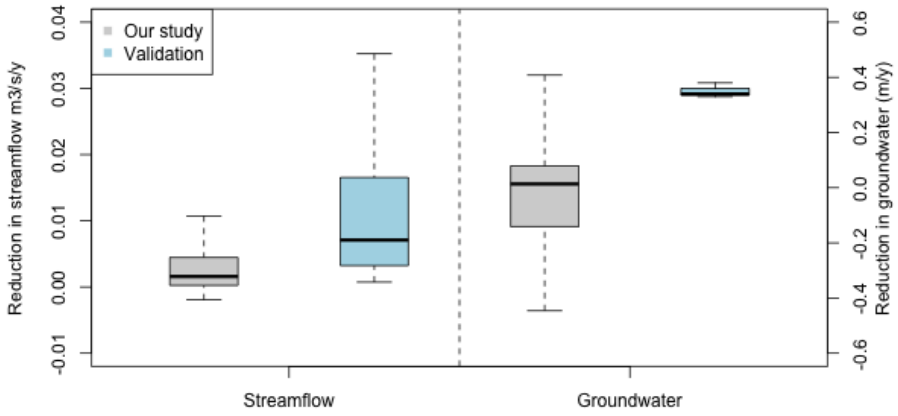

Supplementary Figure S14. Comparison of results of the analytical framework with precipitation-adjusted streamflow trends (18 observations) and groundwater head trends (3 observations) estimated from observations in the Republican River (Wen and Chen, 2006); left panel: box plots of streamflow decline rate ($m^3\ s^{-1}\ yr^{-1}$); right panel: box plot of groundwater head decline rate ($m\ yr^{-1}$); note that in the analytical framework we take $q > q_{crit}$, $t > t_{crit}$ or $q < q_{crit}$, $t >> t_{ef}$ for streamflow and $q > q_{crit}$, $t > t_{crit}$ *for groundwater.*

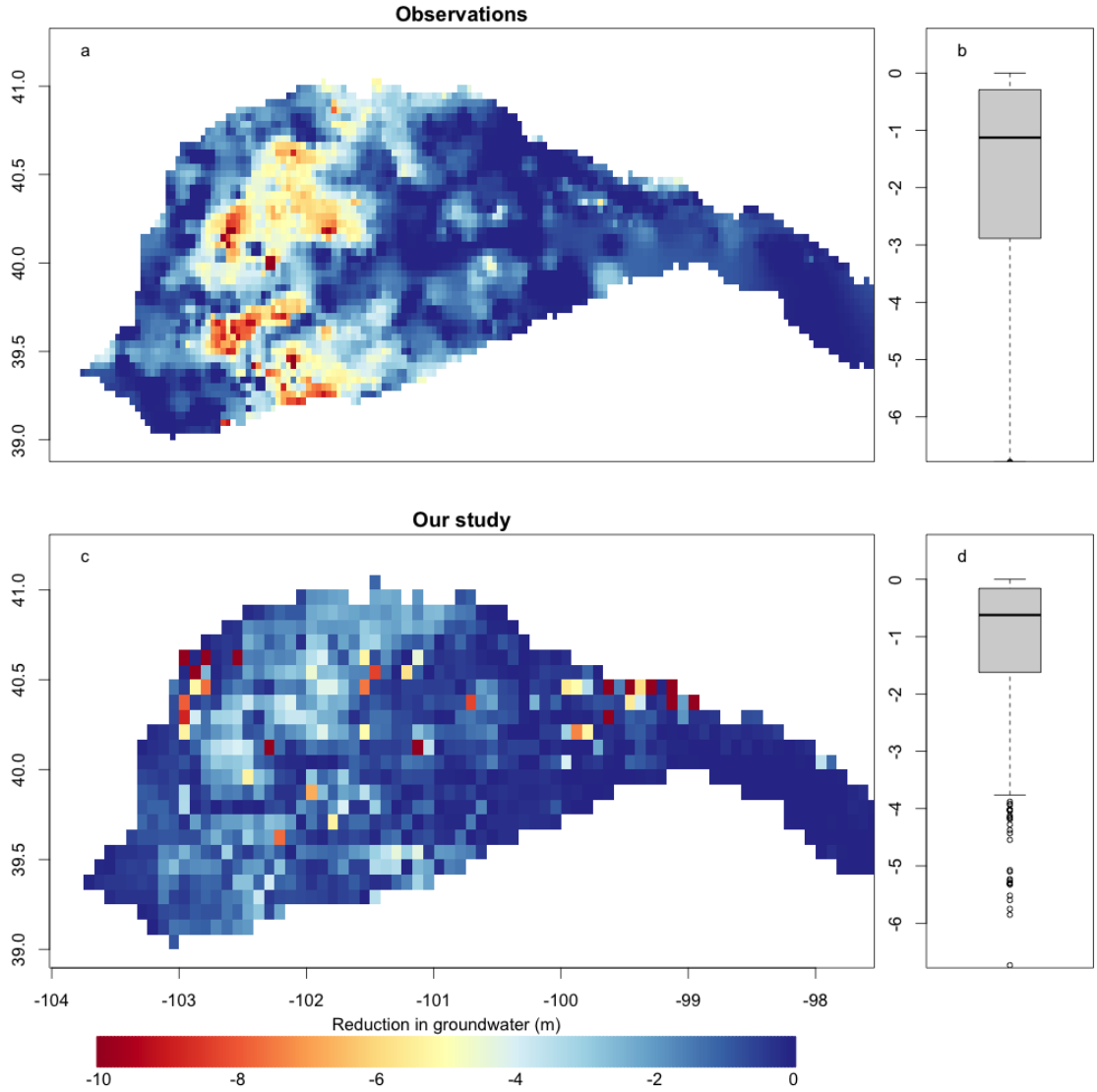

Supplementary Figure S15. Comparison of head declines (m) over the period 2002-2015 from 1522 observation wells in the Republican River (McGuire, 2017) with head decline rates from the analytical framework; (a) interpolated map of head decline from the 1522 observation wells; (b) box plot of head declines at the 1522 observation wells; (c) map of head decline from the analytical framework; (d) box plots of estimated head declines at the 5-arcminute grid cells from the analytical framework; note that in the analytical framework we take $q > q_{crit}$, $t > t_{crit}$.

Supplementary references

Condon, L.E. and Maxwell, R.M.: Simulating the sensitivity of evapotranspiration and streamflow to large-scale groundwater depletion, *Sci. Adv.*, 5, eaav4574, https://doi.org/10.1126/sciadv.aav4574, 2019.

de Graaf, I.E.M., Gleeson, T., van Beek, L.P.H., Sutanudjaja, E.H. and Bierkens, M.F.P. Environmental flow limits to global groundwater pumping, *Nature* 574, 90-108, 2019.

McGuire, V.L.: *Water-level changes in the High Plains aquifer, Republican River Basin in Colorado, Kansas, and Nebraska, 2002 to 2015 (ver. 1.2, March 2017)*, U.S. Geological Survey Scientific Investigations Map 3373, 10 p., 1 sheet with appendix, https://doi.org/10.3133/sim3373, 2017.

Sutanudjaja, E. H., van Beek, R., Wanders, N., Wada, Y., Bosmans, J. H. C., Drost, N., van der Ent, R. J., de Graaf, I. E. M., Hoch, J. M., de Jong, K., Karssenberg, D., López López, P., Peßenteiner, S., Schmitz, O., Straatsma, M. W., Vannametee, E., Wisser, D., and Bierkens, M. F. P.: PCR-GLOBWB 2: a 5 arcmin global hydrological and water resources model, *Geosci. Model Dev.*, 11, 2429–2453, 2018.

Wen, F. and Chen, X.: Evaluation of the impact of groundwater irrigation on streamflow in Nebraska, *J. Hydrol.*, 327, 603-617, 2006.